20. A. Becker *et al.*, *Nat. Struct. Mol. Biol.* **6**, 969–975 (1999).
21. Y. Peng, S. E. Veneziano, G. D. Gillispie, J. B. Broderick, *J. Biol. Chem.* **285**, 27224–27231 (2010).
22. W. Lubitz, H. Ogata, O. Rüdiger, E. Reijerse, *Chem. Rev.* **114**, 4081–4148 (2014).
23. G. E. Cutsail III, J. Telser, B. M. Hoffman, *Biochim. Biophys. Acta* **1853**, 1370–1394 (2015).
24. H.-I. Lee *et al.*, *J. Am. Chem. Soc.* **126**, 9563–9569 (2004).
25. W. Xu *et al.*, *Biochemistry* **51**, 4835–4849 (2012).
26. I. Span *et al.*, *J. Am. Chem. Soc.* **136**, 7926–7932 (2014).

ACKNOWLEDGMENTS

This work was funded by the NIH (grant GM 111097 to B.M.H. and grant GM 54608 to J.B.B.). We thank B.-H. Huynh and C. Krebs for contributions in the early stages of this study.

SUPPLEMENTARY MATERIALS

www.sciencemag.org/content/352/6287/822/suppl/DC1
Materials and Methods
Supplementary Text
Figs. S1 to S3
References (*27*–*39*)

29 February 2016; accepted 29 March 2016
10.1126/science.aaf5327

ATMOSPHERIC SCIENCE

Empirical evidence of contrasting soil moisture–precipitation feedbacks across the United States

Samuel Tuttle* and Guido Salvucci

Soil moisture influences fluxes of heat and moisture originating at the land surface, thus altering atmospheric humidity and temperature profiles. However, empirical and modeling studies disagree on how this affects the propensity for precipitation, mainly owing to the difficulty in establishing causality. We use Granger causality to estimate the relationship between soil moisture and occurrence of subsequent precipitation over the contiguous United States using remotely sensed soil moisture and gauge-based precipitation observations. After removing potential confounding effects of daily persistence, and seasonal and interannual variability in precipitation, we find that soil moisture anomalies significantly influence rainfall probabilities over 38% of the area with a median factor of 13%. The feedback is generally positive in the west and negative in the east, suggesting dependence on regional aridity.

Land-surface moisture content affects the partitioning of radiative energy into latent and sensible heat fluxes (*1*) and therefore can affect the state of the overlying atmosphere by supplying water vapor, inducing moist convection and lateral convergence, and growing the planetary boundary layer (*2*). Previous studies have recognized that soil water content can modify atmospheric processes on a range of spatial and temporal scales (*1*, *3*), potentially leading to cloud formation (*4*) and precipitation (*2*, *5*). In extreme cases, soil moisture may indirectly influence atmospheric circulation (*6*). It is important that the soil moisture–precipitation relationship is characterized, as it has implications for adaptations to future climate change and our ability to forecast weather and make climate projections. For instance, a positive feedback between soil moisture and precipitation could increase the duration of severe dry and wet periods (i.e., droughts and floods), as drier soils would lead to lower precipitation likelihood, and vice versa.

However, the nature of the soil moisture–precipitation relationship is still debated. Past observational and reanalysis studies have indicated that it varies by location, but some analyses have led to disagreements on feedback sign, strength, and statistical significance over the same regions (*5*, *7*–*12*), even using the same data (*13*, *14*). These discrepancies are partly due to the sparse record of soil moisture observations, the different techniques used to identify feedbacks (e.g., temporal versus spatial analyses) (*15*), and the difficulty of distinguishing a causal soil moisture–precipitation effect from lagged correlations that arise from the autocorrelation, seasonality, and interannual variability of each signal (*1*, *14*, *16*, *17*). Modeling studies have been used to circumvent these challenges, with most finding a positive soil moisture–precipitation feedback (*3*, *18*, *19*). However, a wide range of coupling has been found in different models (*18*, *20*), and it has been suggested that land-atmosphere feedbacks are not yet accurately represented (*5*), as convective parameterization and spatial scale may determine not only the feedback strength, but the sign as well (*21*). A review on soil moisture–climate interactions noted the ambiguity in past studies and highlighted the need to identify the causal link between soil moisture and precipitation using observational data (*1*). We believe our results satisfy this need, for the given temporal and spatial scales used here.

Much of the difficulty in determining the nature of soil moisture–precipitation feedback is due to the direct, positive relationship between precipitation and soil moisture in conjunction with the relatively long memory (i.e., autocorrelation) of soil moisture (*1*, *14*–*17*). Precipitation events elevate soil moisture content and may be reflected in the soil moisture record for weeks (*22*) as soil water slowly percolates, evaporates, and is taken up by vegetation. This confounds the observed soil moisture–precipitation relationship by making it difficult to determine whether an increase in precipitation occurrence after a large soil moisture anomaly is a direct effect (i.e., causal), or simply a result of temporal autocorrelation in precipitation, which is then imprinted on soil moisture. To our knowledge, only one previous study (*14*) has sought to directly account for precipitation autocorrelation using statistical causal identification methods (*23*). Others have attempted to address it by incorporating additional information on atmospheric stability (*8*, *10*, *11*); by relating convective triggering to spatial, as opposed to temporal, anomalies in soil moisture (*5*, *15*); by examining covariance with possible confounding variables (*20*); or by stratifying results according to past precipitation (*8*).

We resolve the issue of precipitation autocorrelation by explicitly including both lagged soil moisture and lagged precipitation in a generalized linear model (GLM) of precipitation occurrence (specifically, a probit model), constructed to diagnose the relationship between soil moisture and the probability of next-day precipitation (*24*). We include both continuous and indicator variables in the regression, which represent a set of climatic, atmospheric, and land-surface processes that could influence precipitation occurrence. These consist of sinusoids that vary on interannual and seasonal time scales (to account for external atmospheric and climatic influences on precipitation; e.g., sea surface temperature, seasonality), binary indicator variables that represent the prior occurrence of precipitation [up to 4 days into the past (*24*)], lagged atmospheric pressure (4 days into the past), and previous-day soil moisture (for simple example models, see Fig. 1). The indicator variables account for precipitation persistence from synoptic weather systems (where precipitation events may span multiple days), plus any other source of short-term precipitation persistence, by allowing the regression to predict higher probability of precipitation on days following precipitation. Because this increased probability is statistically accounted for by the indicator variables, it is not attributed to soil moisture, eliminating the influence of precipitation autocorrelation on the soil moisture–precipitation feedback signal. Similarly, including lagged pressure accounts for atmospheric persistence such as drying during lingering high-pressure systems, and seasonal and interannual sinusoids in the regression eliminate the confounding effect of low-frequency correlations of soil moisture and precipitation (caused simply by water balance) on the potential short-term feedback signal.

Boston University, Boston, MA 02215, USA.
*Corresponding author. Email: stuttle@bu.edu

The soil moisture data used in this study are 0.25° resolution satellite observations from the Advanced Microwave Scanning Radiometer for the Earth Observing System (AMSR-E) (*25*, *26*). The precipitation data are gridded gauge observations from the North American Land Data Assimilation System, Phase 2 (NLDAS-2) (*27*).

Because we do not know a priori which factors will influence the probability of precipitation at any given location, we run a large suite of regressions with all permutations of the variables listed above, other than soil moisture (and pressure). This so-called all possible regressions (APR) method is computationally intensive but superior to stepwise methods. We determine which variables are important for predicting precipitation probability and soil moisture for each 0.25° pixel by selecting the regression model that yields the minimum Akaike information criterion (AIC), which penalizes against the model fit by the number of free parameters included in the model (*24*) (for the number of variables selected at each location, see fig. S1). These models yield predictions of precipitation occurrence and soil moisture derived from climatic factors and precipitation persistence (but not soil moisture). Then, employing Granger causality (*23*), we fit the residual precipitation probability to the residual soil moisture and lagged pressure (*24*), focusing only on days where precipitation did not occur on the previous day to further eliminate precipitation persistence. We also use a block bootstrapping method to correct for bias in the regression coefficients introduced by the endogeneity of soil moisture and precipitation occurrence and to test for statistically significant improvement in prediction capability due to soil moisture (*24*). The difference in predictions between the two models estimates the impact of soil moisture on precipitation probability.

By including terms in the regression that account for interannual and seasonal variations, and atmospheric and precipitation persistence, we expect that we have isolated the causal relationship between soil moisture state and the probability of precipitation [although it is always possible in studies employing Granger causality that the inclusion of some neglected common factor could cause the soil moisture coefficient to lose statistical significance (*20*)]. Accounting for lagged precipitation and low-frequency (i.e., seasonal and interannual) variability frames the analysis as a test of rejecting the null, where the null hypothesis is that soil moisture has no influence on future precipitation, and no precipitation persistence is due to soil moisture–precipitation feedback. It is only rejected if, after removing the confounding effects of precipitation autocorrelation, low-frequency variability, and atmospheric persistence, soil moisture still improves the prediction of future precipitation occurrence. Null testing indicated that the model is not vulnerable to false-positive identification of soil moisture–precipitation feedback (fig. S2). This Granger causality (*23*) framework is capable of detecting (*14*) the presence of a feedback provided that soil moisture dynamics are not entirely determined by precipitation (i.e., they are also influenced by other aspects of weather, such as evapotranspiration).

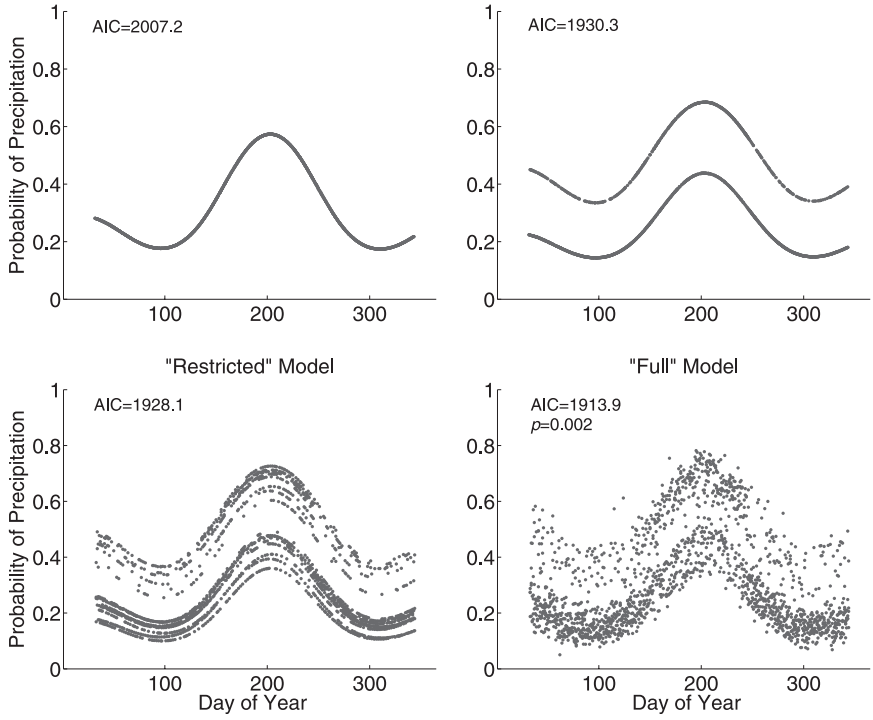

Fig. 1. Example plots illustrating precipitation models of increasing complexity. The plots show probit models of precipitation probability that were fit to observed precipitation occurrence at one location. In each, 9 years of model-estimated precipitation probability are plotted against day of year. In the top left panel, only seasonal terms and a constant were included in the model. In the top right panel, lagged precipitation occurrence was added to the seasonal model. The bottom curve in this panel shows the predicted precipitation probability when precipitation did not occur on the previous day, while the top curve reflects the increased probability predicted by the model when precipitation occurred on the previous day. In the bottom left panel, interannual terms were added to the seasonal-and-persistence model (top right). This is the minimum Akaike information criterion (AIC) (*24*) model for this location, which was determined by regressing all possible combinations of the seasonal, interannual, and lagged precipitation terms on precipitation occurrence [i.e., all possible regressions (APR)]. The model was not required to contain each of these components, but for this location, it contained a constant, two seasonal and two interannual terms, and 1-day lagged precipitation. In the bottom right panel, soil moisture and lagged atmospheric pressure were included, forming the "full" model.

Figure 2 displays the mean soil moisture impact on precipitation probability, for both high and low soil moisture (defined as the mean impact above or below the median seasonally detrended soil moisture anomaly, respectively; see fig. S3) across the United States, for each of two AMSR-E soil moisture products used here (*25*, *26*). The impact is presented as a relative probability factor, reflecting the precipitation probability predicted by the full regression model (i.e., including soil moisture) divided by the precipitation probability predicted without soil moisture. This illustrates the mean degree to which the soil moisture causes the precipitation probability to deviate from its climatological average value, after accounting for persistence and low-frequency variability.

Figure 2 shows a positive feedback of soil moisture on next-day precipitation probability in the western United States and a negative feedback in the east. In general, the areas of positive feedback correspond to more arid regions, whereas more humid, vegetated areas exhibit a negative feedback. Approximately 38% of the United States displays significant feedback (at the 5% significance level), and we find that soil moisture anomalies modify rainfall probabilities by a median factor of 13% (i.e., median absolute impact across all significant pixels in the four panels of Fig. 2). The impact magnitudes differ somewhat between the two AMSR-E soil moisture products, but the sign of the feedback (i.e., positive, negative, or insignificant) agrees over 58% of the study area, and both display an obvious east-negative, west-positive pattern. This same general pattern arises when the analysis period is restricted to individual seasons (fig. S4), or when the data are averaged to larger spatial scales (fig. S5), and is observed in land-surface models (LSMs) forced by the same precipitation data (fig. S6).

Soil moisture–precipitation feedback is not significant over much of the study area, including the Great Plains (a transitional zone between arid and humid regions), where previous modeling studies indicated a "hot spot" of strong land-atmosphere coupling (*18*, *19*, *28*). Our results indicate that weak soil moisture–precipitation feedback

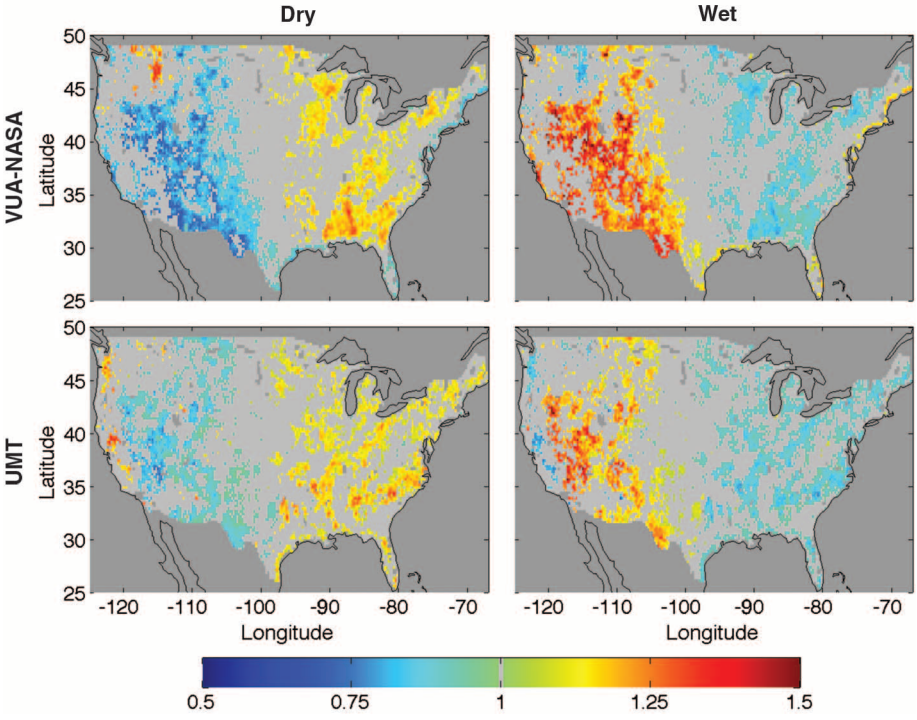

Fig. 2. Maps of the impact of soil moisture on the probability of next-day precipitation. Relative probability factors that represent the mean impact of soil moisture on precipitation probability, calculated as the predicted precipitation probability when soil moisture was included in the regression model divided by the predicted precipitation probability when soil moisture was removed, are shown. Blue colors indicate that the inclusion of soil moisture in the model reduced the predicted precipitation probability, while red colors indicate that the probability increased. Light gray areas denote the absence of a statistically significant relationship (α = 0.05), and dark gray areas were not tested. The values shown are for VUA-NASA (*25*) (top row) and UMT (*26*) (bottom row) soil moisture. The left column shows mean relative impact below median soil moisture anomaly (i.e., drier than seasonal median conditions), and mean relative impact above median soil moisture anomaly (i.e., wetter than seasonal median conditions) is presented in the right column. Negative feedback (i.e., impact higher than 1 in dry soil moisture conditions and lower than 1 in wet conditions) dominates the eastern portion of the study area, while positive feedback (i.e., impact higher than 1 in wet conditions and lower than 1 in dry conditions) is more prominent in western areas.

exists in these areas, after accounting for climatic factors and removing the effects of persistence. We do not find evidence of a strong feedback that varies between positive and negative in sign on a seasonal basis (fig. S4), which could have resulted in temporal cancellation (*9*). Although soil moisture is both highly variable and limits evapotranspiration in this transition zone (*19*), the absence of a feedback indicates that evapotranspiration may not strongly influence precipitation (*11*). Much of the precipitation in the Great Plains occurs during the night (fig. S7) as a result of remotely triggered, eastward-propagating convective systems (*29*), so it is possible that local land-atmosphere interaction is not important for predicting precipitation in this region.

Nevertheless, our results are consistent with a recent observational study (*5*) that found convective initiation over drier soils (i.e., a negative feedback) in limited areas of the eastern United States, and no clear signal in the Great Plains, as well as another study (*10*) that found mostly insignificant feedbacks in the Upper Midwest using atmospheric profiles to filter the relationship between observed precipitation and modeled soil moisture. The east-negative, west-positive pattern in Fig. 2 is quite similar to those found using a feedback strength parameter in monthly evapotranspiration and precipitation reanalysis data (*12*). Another study (*9*) found rank correlations between soil moisture and the lifting condensation level in observations and some models, which spatially agree with our findings of strong positive impact in the west and an abrupt decrease in impact east across the Midwest.

However, the pattern detected here is opposite of that found in studies that used a boundary layer model and sounding data to diagnose areas likely to display positive and negative feedbacks (*7*), and in a study relating morning evaporative fraction and afternoon precipitation from reanalysis data (*11*). When the latter technique is expanded to observational data, the agreement is marginally better, but lack of adequate control for precipitation persistence may still be an issue (*8*).

We emphasize that the results of this analysis only reflect soil moisture–precipitation feedback at a daily timestep and 0.25° spatial scale (and larger, fig. S5) and are dependent on satellite and gridded precipitation data quality. Our conclusions include a number of qualifications. First, this study identifies local feedbacks using a temporal analysis, but does not consider spatial effects [e.g., (*5*, *15*)]. Second, in areas of dense vegetation [e.g., east of the Mississippi River (*9*)], the soil moisture signal detected by AMSR-E may be contaminated and obscured by vegetation (supplementary text and fig. S8). Third, the applied method (*24*) is an effective way to ensure against false positives (e.g., fig. S2), but like any conservative-null approach, it reduces statistical power, thereby increasing the possibility of not identifying a soil moisture–precipitation feedback where one exists.

Fourth, this analysis investigates the probability of precipitation occurrence independent of time of day, which differs from some other studies [e.g., (*5*, *8*, *11*, *15*)] that focused on afternoon precipitation. An assessment of feedback as a function of time of day would be a valuable follow-up investigation, but would require longer data records.

Finally, because the model allows for up to five sinusoidal frequencies to represent the seasonal cycle of precipitation occurrence, the model can adequately represent complex climatological mean patterns. However, other procedures such as window averages could potentially capture sharper transitions.

This analysis does not identify specific mechanisms for soil moisture–precipitation feedback, which are likely a complex interplay between atmospheric and land-surface moisture sources (*8*), boundary layer processes, atmospheric stability (*4*), and possibly nonlocal effects or wind (*30*). However, the opposing results in humid versus arid areas could indicate that the feedback may be different in different climates. The results shown here are consistent with the hypothesis that a lack of atmospheric moisture may be the limiting factor for precipitation in more arid areas [i.e., moisture recycling (*31*)], whereas in humid areas, where atmospheric moisture is abundant, the feedback may be controlled by more dynamic mechanisms [e.g., dampened instability (*32*), or convection triggered by thermal buoyancy over relatively drier soils, or mesoscale convergence (*2*, *3*, *5*)].

This study supports the concept of soil moisture–atmosphere feedback and indicates that knowledge of soil moisture can help to constrain the probability of next-day precipitation in many areas, independently of any precipitation persistence. Further study on boundary layer processes is needed to tease out the physical pathways behind the results shown here, so that these hydrologic relationships may be better represented in weather and climate models.

REFERENCES AND NOTES

1. S. I. Seneviratne *et al.*, *Earth Sci. Rev.* **99**, 125–161 (2010).
2. R. A. Pielke Sr., *Rev. Geophys.* **39**, 151–177 (2001).
3. C. M. Taylor *et al.*, *Nat. Geosci.* **4**, 430–433 (2011).

4. M. B. Ek, A. A. M. Holtslag, *J. Hydrometeorol.* **5**, 86–99 (2004).
5. C. M. Taylor, R. A. M. de Jeu, F. Guichard, P. P. Harris, W. A. Dorigo, *Nature* **489**, 423–426 (2012).
6. E. M. Fischer, S. I. Seneviratne, P. L. Vidale, D. Lüthi, C. Schär, *J. Clim.* **20**, 5081–5099 (2007).
7. K. L. Findell, E. A. B. Eltahir, *J. Hydrometeorol.* **4**, 570–583 (2003).
8. B. P. Guillod *et al*., *Atmos. Chem. Phys.* **14**, 8343–8367 (2014).
9. C. R. Ferguson, E. F. Wood, R. K. Vinukollu, *J. Hydrometeorol.* **13**, 749–784 (2012).
10. L. Alfieri, P. Claps, P. D'Odorico, F. Laio, T. M. Over, *J. Hydrometeorol.* **9**, 280–291 (2008).
11. K. L. Findell, P. Gentine, B. R. Lintner, C. Kerr, *Nat. Geosci.* **4**, 434–439 (2011).
12. X. Zeng, M. Barlage, C. Castro, K. Fling, *J. Hydrometeorol.* **11**, 979–994 (2010).
13. K. L. Findell, E. A. B. Eltahir, *Water Resour. Res.* **33**, 725–735 (1997).
14. G. D. Salvucci, J. A. Saleem, R. Kaufmann, *Adv. Water Resour.* **25**, 1305–1312 (2002).
15. B. P. Guillod, B. Orlowsky, D. G. Miralles, A. J. Teuling, S. I. Seneviratne, *Nat. Commun.* **6**, 6443 (2015).
16. J. Wei, R. E. Dickinson, H. Chen, *J. Hydrometeorol.* **9**, 1364–1376 (2008).
17. S. I. Seneviratne, R. D. Koster, *J. Hydrometeorol.* **13**, 404–412 (2012).
18. R. D. Koster *et al*., *J. Hydrometeorol.* **7**, 590–610 (2006).
19. R. D. Koster *et al*., *Science* **305**, 1138–1140 (2004).
20. B. Orlowsky, S. I. Seneviratne, *J. Clim.* **23**, 3918–3932 (2010).
21. C. Hohenegger, P. Brockhaus, C. S. Bretherton, C. Schär, *J. Clim.* **22**, 5003–5020 (2009).
22. P. A. Dirmeyer, C. A. Schlosser, K. L. Brubaker, *J. Hydrometeorol.* **10**, 278–288 (2009).
23. C. W. J. Granger, *Econometrica* **37**, 424–438 (1969).
24. Materials and methods are available as supplementary materials on *Science* Online.
25. M. Owe, R. A. M. de Jeu, J. Walker, *IEEE Trans. Geosci. Rem. Sens.* **39**, 1643–1654 (2001).
26. L. A. Jones *et al*., A method for deriving land surface soil moisture, vegetation optical depth, and open water fraction from AMSR-E. *Proc. IEEE Geosci. Remote Sens. Symp. (IGARSS 2009), Cape Town, South Africa*. **3**, III-916-III-919 (2009).
27. K. E. Mitchell *et al*., *J. Geophys. Res.* **109**, D07S90 (2004).
28. R. Mei, G. Wang, *J. Hydrometeorol.* **13**, 1010–1022 (2012).
29. R. E. Carbone, J. D. Tuttle, *J. Clim.* **21**, 4132–4146 (2008).
30. P. Froidevaux, L. Schlemmer, J. Schmidli, W. Langhans, C. Schär, *J. Atmos. Sci.* **71**, 782–799 (2014).
31. J. A. Eddy, C. K. Stidd, W. B. Fowler, J. D. Helvey, *Science* **188**, 279–281 (1975).
32. F. Giorgi, L. O. Mearns, C. Shields, L. Mayer, *J. Clim.* **9**, 1150–1162 (1996).

ACKNOWLEDGMENTS

Thanks to P. Dirmeyer and two anonymous reviewers for constructive comments that helped to strengthen this analysis. The data used in this study are freely available online from the NASA Goddard Earth Sciences (GES) Data and Information Services Center (DISC) (http://disc.sci.gsfc.nasa.gov/hydrology), the National Snow and Ice Data Center (NSIDC) Distributed Active Archive Center (DAAC) (http://nsidc.org/data/nsidc-0451), and the Oak Ridge National Laboratory (ORNL) DAAC for biogeochemical dynamics (https://daac.ornl.gov/NACP/guides/NBCD_2000_V2.html). This research was funded by NASA under grant NNX12AP78G (to G.S.).

SUPPLEMENTARY MATERIALS

www.sciencemag.org/content/352/6287/825/suppl/DC1
Materials and Methods
Supplementary Text
Figs. S1 to S8
References (*33*–*51*)

18 January 2015; accepted 4 April 2016
10.1126/science.aaa7185

HIV-1 ANTIBODIES

Fusion peptide of HIV-1 as a site of vulnerability to neutralizing antibody

Rui Kong,[1]* Kai Xu,[1]* Tongqing Zhou,[1]* Priyamvada Acharya,[1] Thomas Lemmin,[2] Kevin Liu,[1] Gabriel Ozorowski,[3,4,5] Cinque Soto,[1] Justin D. Taft,[1] Robert T. Bailer,[1] Evan M. Cale,[1] Lei Chen,[1] Chang W. Choi,[1] Gwo-Yu Chuang,[1] Nicole A. Doria-Rose,[1] Aliaksandr Druz,[1] Ivelin S. Georgiev,[1] Jason Gorman,[1] Jinghe Huang,[6] M. Gordon Joyce,[1] Mark K. Louder,[1] Xiaochu Ma,[7] Krisha McKee,[1] Sijy O'Dell,[1] Marie Pancera,[1] Yongping Yang,[1] Scott C. Blanchard,[8] Walther Mothes,[7] Dennis R. Burton,[9,10] Wayne C. Koff,[11] Mark Connors,[6] Andrew B. Ward,[3,4,5] Peter D. Kwong,[1]† John R. Mascola[1]†

The HIV-1 fusion peptide, comprising 15 to 20 hydrophobic residues at the N terminus of the Env-gp41 subunit, is a critical component of the virus-cell entry machinery. Here, we report the identification of a neutralizing antibody, N123-VRC34.01, which targets the fusion peptide and blocks viral entry by inhibiting conformational changes in gp120 and gp41 subunits of Env required for entry. Crystal structures of N123-VRC34.01 liganded to the fusion peptide, and to the full Env trimer, revealed an epitope consisting of the N-terminal eight residues of the gp41 fusion peptide and glycan N88 of gp120, and molecular dynamics showed that the N-terminal portion of the fusion peptide can be solvent-exposed. These results reveal the fusion peptide to be a neutralizing antibody epitope and thus a target for vaccine design.

Type 1 viral fusion machines, including HIV-1 envelope glycoprotein (Env), mediate virus entry through structural rearrangements that drive virus-cell membrane fusion (*1*–*3*). The hydrophobic N-terminal region of the gp41 transmembrane subunit (the fusion peptide), which is liberated by cleavage of the envelope precursor, is a critical element in this process because it directly interacts with the target-cell membrane in both intermediate and postfusion states (*1*–*3*). In the prefusion state, sequestration of the HIV-1 Env fusion peptide has been thought essential to avoid its being snared by the viral membrane or forming a hydrophobic aggregate with other fusion peptides. Published structures of trimeric HIV-1 Env in its prefusion closed state indicated a surface-exposed fusion peptide located in the membrane-proximal quartile of the viral spike (*4*–*6*); however, substantial disorder of the N-terminal portion of the fusion peptide in both antibody-bound and ligand-free crystal structures (*6*, *7*) made exposure of the fusion peptide unclear.

A chronically HIV-1–infected individual, donor N123 (*8*, *9*), displayed potent serum neutralization (fig. S1A); however, the epitope specificity of the serum-neutralizing antibodies could not be clearly categorized (fig. S1, B and C). We performed antigen-specific single memory B cell sorting with the BG505 SOSIP.664 trimer (*6*, *10*, *11*); among 92 antigen-specific B cells were 7 members of the clonal lineage N123-VRC34 (named for donor "N123" and antibody lineage "VRC34," with specific clone "x" referred to as VRC34."x") (Fig. 1A and fig. S2). The most potent member of the clonal family (VRC34.01) neutralized 16 out of 22 HIV-1 Env-pseudoviruses, including BG505 (fig. S3), and further neutralized 49% of 208 HIV-1 strains (fig. S4 and database S1). VRC34.01 and clonal members bound to BG505 SOSIP.664, but not BG505 gp120 monomer in enzyme-linked immunosorbent assay (ELISA) (Fig. 1B and fig. S5A), and VRC34.01-04, but not VRC34.05-07, bound to cell-surface BG505 trimer (fig. S5, B and C). In competition ELISA, VRC34.01 was partially inhibited by antibody PGT151 (*12*) (fig. S6), and on a panel of 28 glycan mutants of strain BG505, VRC34.01 displayed a profile distinct from PGT151 (fig. S7). VRC34.01 neutralization was reduced by elimination of the N88 glycan and was enhanced by glycan mutations N611Q and N611D. There was minimal effect on VRC34.01 neutralization when viruses were grown in the presence of glycosylation inhibitors kifunensine, swainsonine, or in GnTI$^{-/-}$ cells (fig. S8), suggesting that VRC34.01

[1]Vaccine Research Center, National Institute of Allergy and Infectious Diseases, National Institutes of Health, Bethesda, MD 20892, USA. [2]Department of Pharmaceutical Chemistry, University of California San Francisco, San Francisco, CA, USA. [3]Department of Integrative Structural and Computational Biology, The Scripps Research Institute, La Jolla, CA 92037, USA. [4]Center for HIV/AIDS Vaccine Immunology and Immunogen Discovery, The Scripps Research Institute, La Jolla, CA 92037, USA. [5]International AIDS Vaccine Initiative, Neutralizing Antibody Center, The Scripps Research Institute, La Jolla, CA 92037, USA. [6]HIV-Specific Immunity Section, Laboratory of Immunoregulation, National Institute of Allergy and Infectious Diseases, National Institutes of Health, Bethesda, MD 20892, USA. [7]Department of Microbial Pathogenesis, Yale University School of Medicine, New Haven, CT 06536, USA. [8]Department of Physiology and Biophysics, Weill Cornell Medical College of Cornell University, New York, NY 10021, USA. [9]Department of Immunology and Microbial Science, International AIDS Vaccine Initiative Neutralizing Antibody Center, Center for HIV/AIDS Vaccine Immunology and Immunogen Discovery, The Scripps Research Institute, La Jolla, CA 92037, USA. [10]Ragon Institute of Massachusetts General Hospital, Massachusetts Institute of Technology and Harvard University, Boston, MA 02142, USA. [11]International AIDS Vaccine Initiative, New York, NY 10038, USA.
*These authors contributed equally to this work. †Corresponding author. Email: pdkwong@nih.gov (P.D.K); jmascola@nih.gov (J.R.M)